

Article

Reasonable Energy-Abandonment Operation of a Combined Power Generation System with an Ultra-High Proportion of Renewable Energy

Hao Zhang¹, Jingyue Yang¹, Chenxi Li¹, Pengcheng Guo^{1,*}, Jun Liu², Ruibao Jin², Jing Hu², Fengyuan Gan³ and Fei Cao⁴

¹ School of Water Resources and Hydroelectric Engineering, Xi'an University of Technology, Xi'an 710048, China; hzhang@xaut.edu.cn (H.Z.); 2210421191@stu.xaut.edu.cn (J.Y.); lichenxi@xaut.edu.cn (C.L.)

² Henan Jiaotou Jiaozheng Expressway Co., Ltd., Zhengzhou 450003, China; ljun202404@163.com (J.L.); Zhouhekuan1108@163.com (R.J.); jiayaofei1122@163.com (J.H.)

³ Henan Province Highway Engineering Bureau Group Co., Ltd., Zhengzhou 450000, China; ganfenyuan1106@163.com

⁴ Henan Railway Construction & Investment Group Co., Ltd., Zhengzhou 450046, China; cfei0408@163.com

* Correspondence: guopengcheng0224@163.com

Abstract: With large-scale grid-connected renewable energy, new power systems require more flexible and reliable energy storage power sources. Pumped storage stations play an important role in peak shaving, valley filling, and promoting renewable energy consumption. This paper presents the reasonable energy-abandonment operation of a combined power generation system (CPGS), in which a pumped storage station is the core control power, with an ultra-high proportion of renewable energy. Firstly, based on the seasonal characteristics of wind, solar, and load demand, typical days are selected through improved clustering analysis algorithms. Then, a daily optimal scheduling model for combined power generation systems (CPGS) is developed with the goals of economy, low-carbon, and stable operation. Finally, the correlation between the energy-abandonment rate and pumped storage station peak shaving and system optimization operation indicators is obtained by a reasonable energy-abandonment calculation method considering source-grid-load coordination. Taking the operation data of an energy base in the western region of China as an example, when the penetration rate of renewable energy is 60–70% in the future, the operating cost on the power side is greatly affected by the construction of the source side. When the system operates at a planned reasonable energy-abandonment rate of 2%, electricity regulation, load tracking, and daily operating costs all show better performance.

Keywords: combined power generation system; optimal operation; ultra-high proportion of renewable energy; reasonable energy-abandonment; pumped storage power station



Citation: Zhang, H.; Yang, J.; Li, C.; Guo, P.; Liu, J.; Jin, R.; Hu, J.; Gan, F.; Cao, F. Reasonable Energy-Abandonment Operation of a Combined Power Generation System with an Ultra-High Proportion of Renewable Energy. *Energies* **2024**, *17*, 1936. <https://doi.org/10.3390/en17081936>

Received: 11 March 2024

Revised: 7 April 2024

Accepted: 15 April 2024

Published: 18 April 2024



Copyright: © 2024 by the authors. Licensee MDPI, Basel, Switzerland. This article is an open access article distributed under the terms and conditions of the Creative Commons Attribution (CC BY) license (<https://creativecommons.org/licenses/by/4.0/>).

1. Introduction

In the future power supply of the grid, the proportion of fossil energy will gradually decrease. At the same time, renewable energy sources (volatile renewable energy sources), represented by wind and solar energy, have a lot of room for growth and will gradually replace traditional energy sources. Renewable energy itself has strong volatility and randomness, and the power generated by it relies on power electronic equipment to access the power grid. Power electronic equipment with low immunity, weak support, and zero inertia characteristics will make grid security and stability issues increasingly prominent, and the accumulation of quantitative changes may trigger qualitative changes in the operating characteristics of the grid.

The transformation of the power system requires policy support from governments, grid companies, and power generation companies. The introduction of relevant policies

can accelerate the progress of this process. Plans formulated by governments and grid companies, such as grid parity prices and carbon tax subsidies, can speed up the integration of renewable energy technologies, improve the efficiency of system power generation, and hasten the transition of the power system [1,2].

To ensure the consumption of renewable energy generation, China's National Development and Reform Commission (NDRC) issued the "Full Coverage Mandatory Acquisition Regulation for Renewable Energy Electricity Volume". The regulation states that power grid companies and related electric power institutions must enhance the consumption and efficient utilization of renewable energy according to the relevant provisions of the renewable energy consumption guarantee mechanism while ensuring the safety of the power grid. The grid side must ensure the consumption of the guaranteed acquisition electricity volume of renewable energy generation projects; power dispatch institutions should formulate corresponding power dispatch plans to guarantee the priority dispatch of renewable energy generation.

Regarding the challenges that large-scale utilization of renewable energy poses to power grid systems, there have been demonstrations of application technologies related to large-scale renewable energy utilization and integrated energy systems. Among these, there have been some research achievements in areas such as offshore wind power [3], renewable energy hydrogen production [4], photovoltaic–thermal hybrid systems [5], wind energy thermal utilization [6], and wind–solar-storage integrated energy systems, where renewable energy serves as the main source of electricity and integrated with other energy sources. These developments pave the way for a new pattern of diversified utilization of new energy. Renewable energy technologies can also be integrated into sustainable buildings and urban environments to reduce dependence on fossil fuels. For example, distributed photovoltaics can reduce carbon emissions and improve energy efficiency and recycling [7]. In addition, as China's renewable energy technology develops, the government can accelerate the transition to a new type of power system and mitigate the impacts of climate change by formulating preferential policies related to renewable energy, promoting sustainable development of the economy and the environment [8]. So, with the increase in the proportion of renewable energy, how can we ensure stable and efficient consumption? Is the ultimate goal to realize 100% renewable energy consumption? Where will the inflection point of system consumption occur?

Pumped storage stations, the most developed flexible energy source with outstanding peak shaving and valley filling capabilities [9], can flexibly manage energy supply and demand [10], which is essential for addressing the issue of wind and solar absorption and guaranteeing the secure and reliable functioning of the power system [11]. The study of the optimal scheduling of a combined power generation system (CPGS) with participating pumped storage stations is now a hot topic [12]. Most studies consider economic efficiency [13], power quality [14], and environmental impact [15] to be the primary goals of the optimal scheduling issue.

When it comes to economic advantages, the goal function may be separated into three parts: the greatest comprehensive operational benefit [16,17], the lowest comprehensive operating cost [18–20], and a thorough assessment of system coordination and economy [21,22]. In the context of power quality, the objective function typically pertains to minimizing the generalized load fluctuation and peak-valley difference of the residual load [23] while simultaneously ensuring optimal power output stability [11]. When the primary aim is to achieve environmental sustainability, the objective function primarily takes into account the cost of carbon emissions. In the context of multi-objective optimization, it is common practice to integrate several individual objectives, including but not limited to maximizing economic gains, optimizing power quality, minimizing carbon emissions, and reducing output fluctuations [24–28]. The aforementioned scheduling models for pumped storage stations in the context of combined power generation system from diverse energy sources represent optimal solutions. The outcomes of these solutions demonstrate the

significant contribution of pumped storage stations towards the optimization of combined power generation systems.

Considering the economic and low-carbon operation of the combined power generation system, the problem of renewable energy consumption is also a key issue in the development of the combined power generation system. In the future, the installed capacity of renewable energy will continue to increase, and the power grid operation will continue to increase the risks of large operation fluctuations, load reduction, and power rationing. There are two main reasons for the abandonment of renewable energy: firstly, the grid frame at the end of the power grid is blocked [29], as the output of renewable energy exceeds the transmission capacity of the power grid. The second reason is that the peak regulation of the power supply end is blocked [30], as the renewable energy output exceeds the maximum adjustment range of the system. At present, current research on reasonable energy consumption can be divided into two categories: one is to find the balance point between the cost and benefit of renewable energy consumption [31], and the second goal is to minimize the consumption cost of renewable energy in the entire society [32]. Due to abundant renewable energy resources and large installed capacity in northwest China, the energy-abandonment rate is relatively high [33]. The energy-abandonment rate of wind and solar in Gansu Province was approximately 6% and 2%, respectively, in 2022.

The optimal operation of pumped storage power stations in a multi-energy combined generation system is significantly impacted by the randomness and volatility of the source-load side data during the optimization process. Therefore, when analyzing the flexible potential of pumped storage power stations, it is necessary to fully consider the randomness and fluctuation characteristics of wind power, photovoltaic power, and grid loads, as well as the energy-abandonment rate. Based on this, this article takes an energy base in the western region of China as the research object. The clustering analysis algorithm is used to extract the characteristics of the year-round source load side data of the base. On this basis, a multi-objective optimization scheduling model is developed considering the minimum load fluctuation, total operating cost, and carbon emissions of the combined power generation system. Reasonable energy-abandonment operation of the combined power generation system is analyzed with ultra-high proportion of renewable energy.

The remainder of the study is structured as follows. Section 2 presents the processing of typical daily source-load data for an energy base in the western region of China by the K-means algorithm; Section 3 introduces the modeling of the combined power generation system considering the constraints and objective functions; Section 4 provides the calculation method of reasonable energy-abandonment and the system simulations; Section 5 presents the conclusions and future work.

2. The Selection of a Typical Day Using the K-Means Algorithm

The K-means algorithm is one of the most widely used clustering algorithms, which has the advantage of dividing the input unknown data set into multiple categories according to its internal data characteristics and has the advantage of fast convergence when searching for the local optimal solution. The traditional K-means algorithm needs to set the clustering number k in advance according to the characteristics of the required data. Therefore, this paper selects the point with the largest initial data density of each quarter as the initial clustering center; the points that are farthest from the initial cluster center and satisfy the density condition are selected as the cluster center by iterative calculation. Therefore, this paper intends to use the K-means algorithm to classify historical data affected by the seasonal variation factors of wind power and photovoltaic output. Additionally, the typical days of their output are screened.

Due to the seasonal characteristics of wind power, photovoltaic power, and load, the randomness and peak shaving characteristics of wind power are significant. The correlation between solar radiation and photovoltaic output is strongest. The daily output is relatively regular, and the load demand in winter and summer is relatively high, with consistent changes in output patterns across different seasons. To effectively capture seasonal features

and generate representative typical scenes for the energy base in the western region of China, this article uses the K-means algorithm to divide the scenery and solar output scenes of the four seasons into four groups. The typical days for spring, summer, autumn, and winter are April 17, July 26, October 16, and January 17, respectively.

Figure 1 shows the average daily load curve and solar output curve obtained based on clustering technology. In terms of photovoltaic resources, autumn is particularly abundant. Output began to rise around 8 am, peaked around 1 pm, and reached its lowest point around 6 pm. This model highlights the significant stability and elasticity of output. Compared to photovoltaic resources, wind power generation exhibits significant changes, with significant differences between seasons and throughout the day. Peak production was observed in the early morning (0 am to 3 am) and afternoon of summer. In other seasons, this pattern is relatively consistent, reaching its peak at midnight, followed by a decrease in intensity. It is worth noting that wind power generation exhibits an anti-peak characteristic, with the lowest generation around noon, which is in stark contrast to solar power generation.

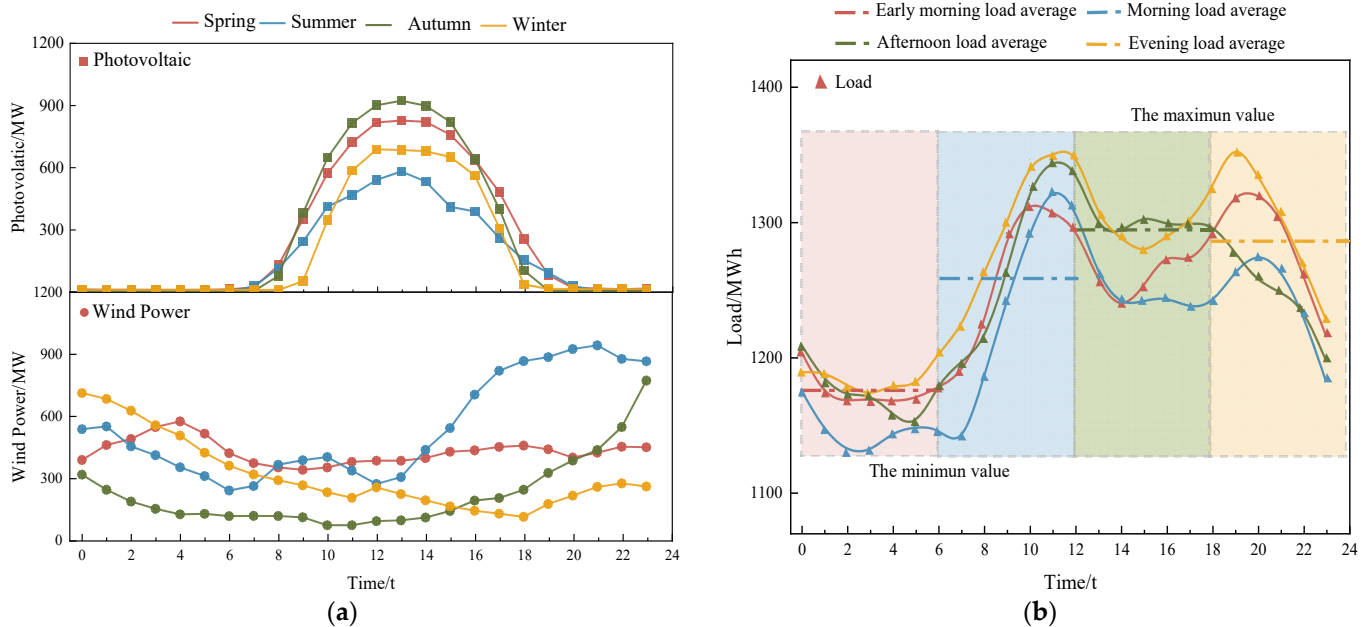


Figure 1. Wind power, PV, and daily load curves of typical days in four seasons. (a) Wind power and photovoltaic output curve. (b) Load demand curve.

As depicted in Figure 1b, a notable nonlinear correlation exists between the daily load across different seasons. The average daily load consistently surpasses 1100 MWh for all seasons at this stage. Notably, during the early hours of the day, the load is minimized, bottoming out around 7 am in spring. Contrary to the trend in the early morning, as the daily average load production nears 1300 MWh, the total daily load starts its ascent as morning progresses. This represents a 7% increase from the early morning demand. By the afternoon, the daily load exhibits fluctuations, initially declining and then climbing, with the average daily load remaining relatively stable compared to the morning values. Come evening, there is a pronounced upward trajectory for the daily load in each season, culminating at its zenith around 7 pm. Specifically, the autumn output peaks at approximately 1362 MWh at 19:00.

Upon conducting a macroscopic evaluation, it has been observed that the disparity between the peak and trough in typical daily load profiles is most pronounced during the summer months. Correspondingly, the pattern of counter-peak regulation by wind power generation is distinctly more evident in this season. This trend is accompanied by a more robust complementarity between wind and solar energy outputs. Consequently, the energy modulation efficacy of pumped storage is markedly enhanced under such typical

daily conditions. In light of these findings, this research will pivot towards an in-depth analysis of representative summer daily load demands and the corresponding wind and solar energy production data to further elucidate this phenomenon.

3. Modeling of the Combined Power Generation System

3.1. Objective Function

This section presents a joint optimal scheduling model for pumped storage–wind–solar–thermal, taking into consideration the objectives of economic efficiency, environmental protection, and operational efficiency. A multi-objective optimal scheduling model is developed to address the power balance constraints of the system, as well as the constraints associated with the operation of wind, photovoltaic, thermal power, and pumped storage. The model aims to minimize the generalized load fluctuation, the operating cost of the joint system, and carbon emission, simultaneously.

The objective function with the least fluctuation in generalized load can be expressed as follows:

$$\min f_1 = \frac{\sum_{t=1}^T (P_{gl,t} - P_{gl,t,av})^2}{T}, \quad (1)$$

$$P_{gl,t} = P_{t,i}^D - P_{t,i}^W - P_{t,i}^{PV} - P_{t,i}^{PH}, \quad (2)$$

$$P_{gl,t,av} = \frac{1}{T} \sum_{i=1}^T P_{gl,t,i}, \quad (3)$$

where $P_{gl,t}$ is the generalized load value in period t , MWh. $P_{gl,t,av}$ is the average of generalized load values, MWh. $P_{t,i}^D$ is the real-time load value in period t , MWh. $P_{t,i}^W$, $P_{t,i}^{PV}$, and $P_{t,i}^{PH}$ represent the generated power of wind power, photovoltaic, and pumped storage in period t respectively, MW.

The objective function with the least operating costs can be formulated as follows:

$$\min f_2 = Z_1 + Z_2 + Z_3 + Z_4, \quad (4)$$

where Z_1 and Z_2 represent the operating cost and the pollution control cost of thermal power units, respectively, \$. Z_3 is the cost of pumped storage pumping in the combined power generation system, \$. Z_4 represents the penalty cost for wind and solar power, \$.

The objective function used to calculate the minimum carbon emissions is as follows:

$$\min f_3 = \sum_{t=1}^T 0.33 \times P_{t,i}^T A_{CO_2}, \quad (5)$$

where $P_{t,i}^T$ is thermal power units output in period t , MW. A_{CO_2} represents the amount of carbon dioxide emitted, kg.

3.2. Constraints

(1) Limits on power balance can be stated as follows:

$$P_{t,i}^T + P_{t,i}^W + P_{t,i}^{PV} + P_{t,i}^{PH} = P_{t,i}^D, \quad (6)$$

where $P_{t,i}^D$ is the real-time load value in period t , MWh. $P_{t,i}^T$ represents the generated power of thermal power units in period t , MW. $P_{t,i}^{PH} < 0$ indicates that the pumped storage power station is in the pumping state; $P_{t,i}^{PH} > 0$ indicates that the pumped storage power station is in a state of power generation.

(2) Constraints of thermal power units

The limitations on the output of thermal power units can be defined as follows:

$$P_{i,\min}^T \leq P_{t,i}^T \leq P_{i,\max}^T \quad (7)$$

where $P_{i,\min}^T$ and $P_{i,\max}^T$ represent the minimum and maximum output of the i thermal power unit, respectively, MW.

The climbing rate constraints of thermal power units can be expressed as follows:

$$-v_{t,i}^{down} \Delta t \leq P_{t,i}^T - P_{(t-1),i}^T \leq v_{t,i}^{up} \Delta t, \quad (8)$$

where $v_{t,i}^{down}$ and $v_{t,i}^{up}$ represent speed limit of the load shedding and load climbing of the i thermal power unit in period t . In this article, the value of Δt is taken as 1 h. $P_{(t-1),i}^T$ represents the generated power of thermal power units in the period immediately preceding period t .

(3) The constraint of wind power output is as follows:

$$0 \leq P_{t,i}^W \leq P_{\max}^W \quad (9)$$

where $P_{t,i}^W$ is the actual output value of wind power in period t , MW. P_{\max}^W is the maximum limit of wind power output, MW.

(4) The constraint of photovoltaic output is as follows:

$$0 \leq P_{t,i}^{PV} \leq P_{\max}^{PV} \quad (10)$$

where $P_{t,i}^{PV}$ is the actual output value of photovoltaic in period t , MW. P_{\max}^{PV} is the maximum limit of photovoltaic output, MW.

(5) Pumped storage power station constraints

The pumped storage power station output constraint can be expressed as follows:

$$0 \leq P_{t,i}^{PH} \leq P_{\max}^{PH} \quad (11)$$

where P_{\max}^{PH} represents the maximum output of pumped storage, MW.

The constraints of working conditions can be divided into energy storage constraints and power generation constraints.

Energy storage constraints can be expressed as follows:

$$P_{gemin} \leq P_{t,i,ge}^{PH} \leq \min\left(P_{gemax}, \frac{E_t}{t} \eta_{ge}\right), \quad (12)$$

$$E_{t+1} = E_t + t(\eta_{ps} P_{t,i,ps}^{PH} - \frac{P_{t,i,ge}^{PH}}{\eta_{ge}}), \quad (13)$$

$$0 \leq E_t \leq E_{\max}, \quad (14)$$

where P_{gemin} and P_{gemax} represent the minimum and maximum output of pumped storage, MW. E_t is upper reservoir stores energy in period t . η_{ps} , η_{ge} represent energy storage and power generation efficiency of pumped storage, respectively. The subscripts ge and ps , respectively, represent the pumped storage unit in generating and pumping states.

Power generation constraint can be expressed as follows:

$$P_{ps,\min}^{PH} \leq P_{t,i,ps}^{PH} \leq P_{ps,\max}^{PH} \quad (15)$$

Pumped storage unit working condition constraint can be expressed as follows:

$$u_{t,i,ps}^{PH} \times u_{t,i,ge}^{PH} \times u_{t,i,st}^{PH} = 0, \quad (16)$$

where $u_{t,i,ps}^{PH}$, $u_{t,i,ge}^{PH}$, $u_{t,i,st}^{PH}$ are 0–1 variables, subscripts representing energy storage, power generation, and static states, respectively.

Single-day draw-out balance constraint can be expressed as follows:

$$\frac{\sum_{t=1}^T P_{t,i,ge}^{PH} \eta_{ge}}{\eta_{ps}} = \sum_{t=1}^T P_{t,i,ps}^{PH}. \quad (17)$$

Upper and lower storage capacity constraints can be expressed as follows:

$$\frac{W_0 - W_{\max}}{\eta_{ps}} \leq \frac{\sum_{t=1}^T P_{t,i,ge}^{PH} \eta_{ge}}{\eta_{ps}} - \sum_{t=1}^T P_{t,i,ps}^{PH} \leq \frac{W_0 - W_{\min}}{\eta_{ps}}, \quad (18)$$

where W_0 is the initial amount of water in the reservoir. W_{\min} , W_{\max} represent minimum and maximum water volumes of the reservoir, respectively.

Unit start–stop constraints can be expressed as follows:

$$u_{t,i,ps}^{PH} + u_{t,i,ge}^{PH} \leq 1, \quad (19)$$

$$K_{t,i,ps}^u - K_{t,i,ps}^d = u_{t,i,ps}^{PH} - u_{(t-1),i,ps}^{PH}, \quad (20)$$

$$K_{t,i,ps}^u + K_{t,i,ps}^d \leq 1, \quad (21)$$

$$K_{t,i,ge}^u - K_{t,i,ge}^d = u_{t,i,ge}^{PH} - u_{(t-1),i,ge}^{PH}, \quad (22)$$

$$K_{t,i,ge}^u + K_{t,i,ge}^d \leq 1, \quad (23)$$

$$\max\{K_{t,i,ge}^u, K_{t,i,ge}^d\} \leq N_{ge}, \quad (24)$$

$$\max\{K_{t,i,ps}^u, K_{t,i,ps}^d\} \leq N_{ps}, \quad (25)$$

$$u_{t,i,ps}^{PH} \leq (N - 1) \left(1 - u_{t,i,ge}^{PH}\right), \quad (26)$$

where $K_{t,i,ps}^u$, $K_{t,i,ps}^d$, $K_{t,i,ps}^u$, $K_{t,i,ps}^d$ are 0–1 variables of start–stop actions of the pumped storage unit under energy storage and power generation conditions, respectively. N_{ge} , N_{ps} are the maximum number of daily starts and stops of pumped storage units under power generation and energy storage conditions, respectively.

(6) The process of linearizing thermal power constraints

In the computation of operating costs for thermal power units, the coal consumption cost is modeled as a quadratic function. However, directly multiplying the constant of the quadratic term can result in significant errors. Additionally, due to the large number of nodes in the unit combination, solving the problem using this method can be time-consuming. Thus, to streamline the solution process and simplify the methodology, the nonlinear quadratic function pertaining to the coal consumption cost of thermal power units is transformed into a linear function. The approach is illustrated in Figure 2.

The original model is replaced with Equation (27) after linearizing the coal consumption function in segments and dividing it into five segments.

$$C_i(P_{t,i,s}, u_{i,t}) = \sum_{s=1}^5 K_{i,s} P_{t,i,s} + u_{t,i} C_{0,i}, \quad (27)$$

$$\begin{cases} C_{t,i,0} = a_{ti,0}P_{i,\min}^2 + b_{ti,0}P_{i,\min} + c_{ti} \\ 0 \leq P_{t,i,s} \leq \frac{P_{i,\max} - P_{i,\min}}{5} \\ P_{t,i} = \sum_{s=1}^5 P_{t,i,s} + P_{i,\min} \end{cases}, \quad (28)$$

where $K_{i,s}$ is the slope of each segment of the coal consumption function after piecewise linearization. $C_{ti,0}$ represents the coal consumption generated by the thermal power unit operating at minimum output, \$. $P_{t,i,s}$ is the output of thermal power unit segments, MW.

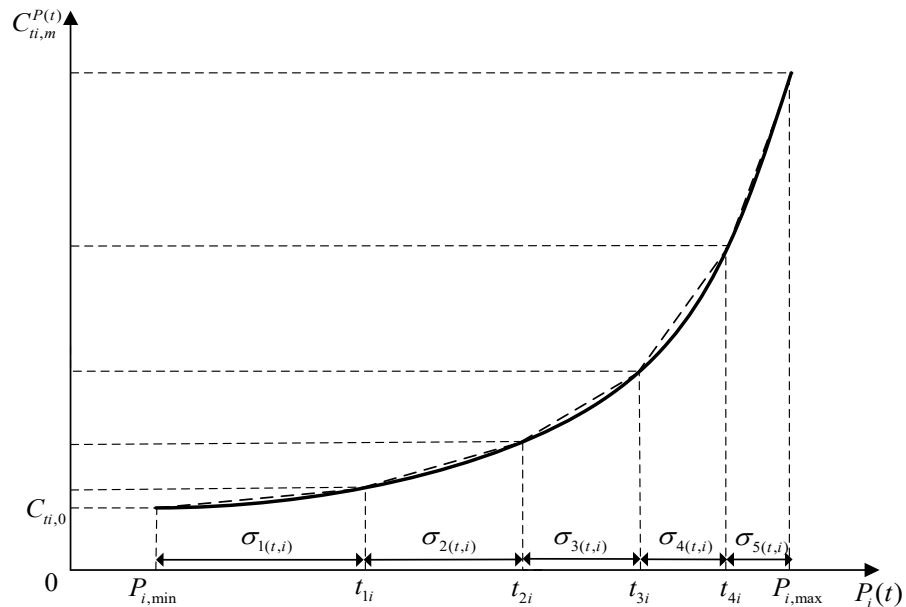


Figure 2. Piecewise linearized curve of the fuel cost for thermal power units.

4. Ultra-High Proportion Renewable Energy Access System

4.1. Calculation Method of Reasonable Energy-Abandonment

This study utilizes the pertinent parameters of the energy base in the western region of China as the foundation for analysis. The pumped storage station is equipped with four reversible pump turbine units that have a power rating of 300 MW. On average, this power station has a water-to-electricity conversion efficiency of 75%.

In the future, with the explosive growth of renewable energy installations, the high proportion of renewable energy and the withdrawal of traditional energy sources will exacerbate the difficulties in grid operation, transmission, and dispatch. The energy-abandonment rate of renewable energy will also rise further. Therefore, reducing the energy-abandonment rate and improving the stability of power grid operation by allocating reasonable peak shaving capacity have become key issues.

It is important to calculate the comprehensive cost curve between the power source and both sides of the power grid under different energy-abandonment rates. When the renewable energy generation on the power supply side remains constant, the system primarily increases the output of renewable energy by increasing its installed capacity. When the grid side’s consumption capacity for renewable energy generation remains stable, the main approach is to improve the grid structure and introduce new peak-shaving power sources to reduce the energy-abandonment rate. The current phase marks the early transition to a new type of power system characterized by a relatively small installed capacity of renewable energy on the power supply side. As the installed capacity of renewable energy increases in the future, the cost on the source side shows an exponential upward trend. Due to the introduction of flexible adjustable power sources in the early stage, the construction investment cost on the power grid side is relatively high. Therefore, as the energy-abandonment rate increases, the cost decrease shows a rapid to gradual trend. The comprehensive cost curve roughly presents a “concave” shape, and its valley

value corresponds to the reasonable energy-abandonment rate of the combined power generation system.

The comprehensive cost composition of the system considered in this article is shown in Figure 3. The schematic diagram of reasonable energy-abandonment points for the combined power generation system under different energy-abandonment rates is shown in Figure 4.

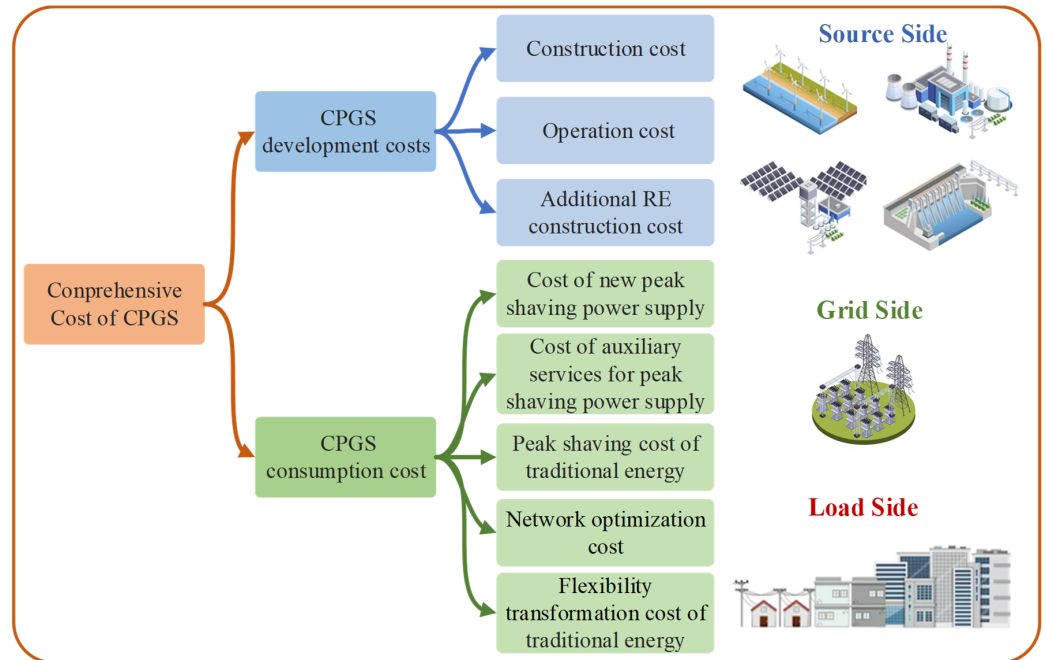


Figure 3. Comprehensive cost composition of the combined power generation system (CPGS).

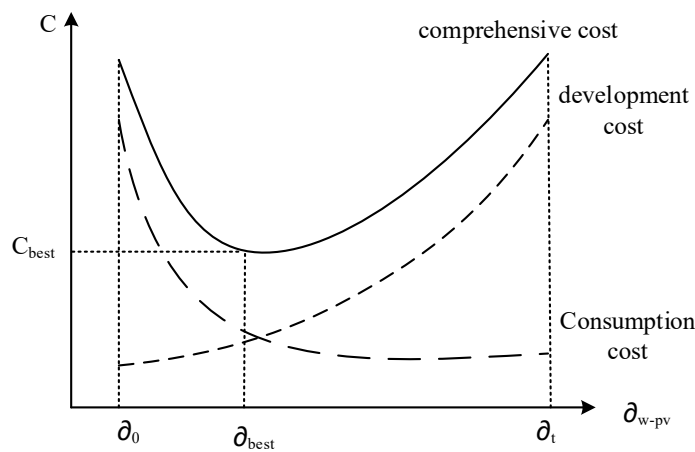


Figure 4. Comprehensive cost of the system under different energy-abandonment rates.

This section considers the cost balance between the power source side and the grid side as the energy-abandonment rate point for the combined power generation system, and its expression is as follows.

$$C_{best} = \min f(\partial_{w-pv}) = f(\partial_{best}) = \min(C_d + C_c) \tag{29}$$

In the formula, C_{best} is the minimum value of the comprehensive cost of the system. In other words, within the function that describes the relationship between the energy-abandonment rates and the comprehensive cost, the obtained minimum value of the integrated cost corresponds to the most reasonable energy-abandonment rate ∂_{best} ; ∂_{w-pv}

represents energy-abandonment rate; $f(\partial_{w-pv})$ is the functional relationship between the energy-abandonment rate and the comprehensive cost.

The development cost of source side energy mainly includes the daily average investment in renewable energy installation C_{Con} , the daily operating cost of the system under different energy-abandonment rates C_{Ope} , and the cost of new energy construction C'_{Con} .

$$C_d = C_{Con} + C_{Ope} + C'_{Con}. \quad (30)$$

The investment in renewable energy installation is the daily average of the annual value of renewable energy investment, calculated at USD 980/kW for wind power and USD 588/kW for photovoltaic power, respectively.

$$C_{Con} = \frac{\text{avg} \sum_{i=1}^2 C_{con}^i \times \left[\frac{r_i \times (1+r_i)^{n_i}}{(1+r_i)^{n_i} - 1} \right]}{N}. \quad (31)$$

In the formula, $i = 1, 2$ represents wind power, and photovoltaic power C_{con}^i , r_i , n_i , N are investment, withdrawal rate, operating years, and annual operating days.

To improve system consumption on the grid side, it is necessary to consider the cost of a newly built pumped storage power plant to solve system peak shaving problems, \$. C_{cha} is the pumping cost of pumped storage power plants during peak shaving, \$. $C_{t,i,0}$ is the coal cost of thermal power plants participating in peak shaving, \$. C_{str} is the flexibility transformation cost of existing thermal power plants, \$, and C_{fle} is the network optimization cost of the power grid to enhance transmission capacity, \$.

$$C_c = C_{con,ps} + C_{cha} + C_{t,i,0} + C_{str} + C_{fle}. \quad (32)$$

The development of the pumped storage power station will serve the renewable energy base in the western region of China. In the future, it is necessary to study how to optimize the operation of pumped storage as a regulating power source for combined power generation systems and how to carry out reasonable energy abandonment in the case of an ultra-high proportion of new energy access.

4.2. Reasonable Energy-Abandonment Operation of the System

According to the development requirements of the renewable energy base in the western region of China, the access system for thermal power and the pumped storage power station is set with the same capacity and regulation capacity, and the penetration rate of renewable energy is over 50%. This means studying the consumption problem of ultra-high proportion renewable energy access systems when the peak shaving power capacity is constant. Under the condition of limited peak shaving power supply, as the penetration rate of renewable energy continues to increase, considering both sides of source and grid, and considering the issue of reasonable energy-abandonment rate, the impact of the proportion of renewable energy connected to the system and the energy-abandonment rate on the cost of the combined power generation system is studied. The capacity of connected renewable energy is set as shown in Table 1.

Table 1. Capacity configuration schemes in different scenarios.

Scenario	Wind Power (MW)	Photovoltaic (MW)	Thermal (MW)	Pumped Storage (MW)	Renewable Energy Penetration Rate
Scenario 1	1500	1300	800	1200	0.58
Scenario 2	2000	1800	800	1200	0.65
Scenario 3	2500	2300	800	1200	0.70
Scenario 4	3000	2800	800	1200	0.74
Scenario 5	3500	3200	800	1200	0.77

For the combined power generation system with an ultra-high proportion of renewable energy integration, different energy-abandonment rates are set for each scenario, and the daily scheduling curve of each scenario is shown in Figure 5.

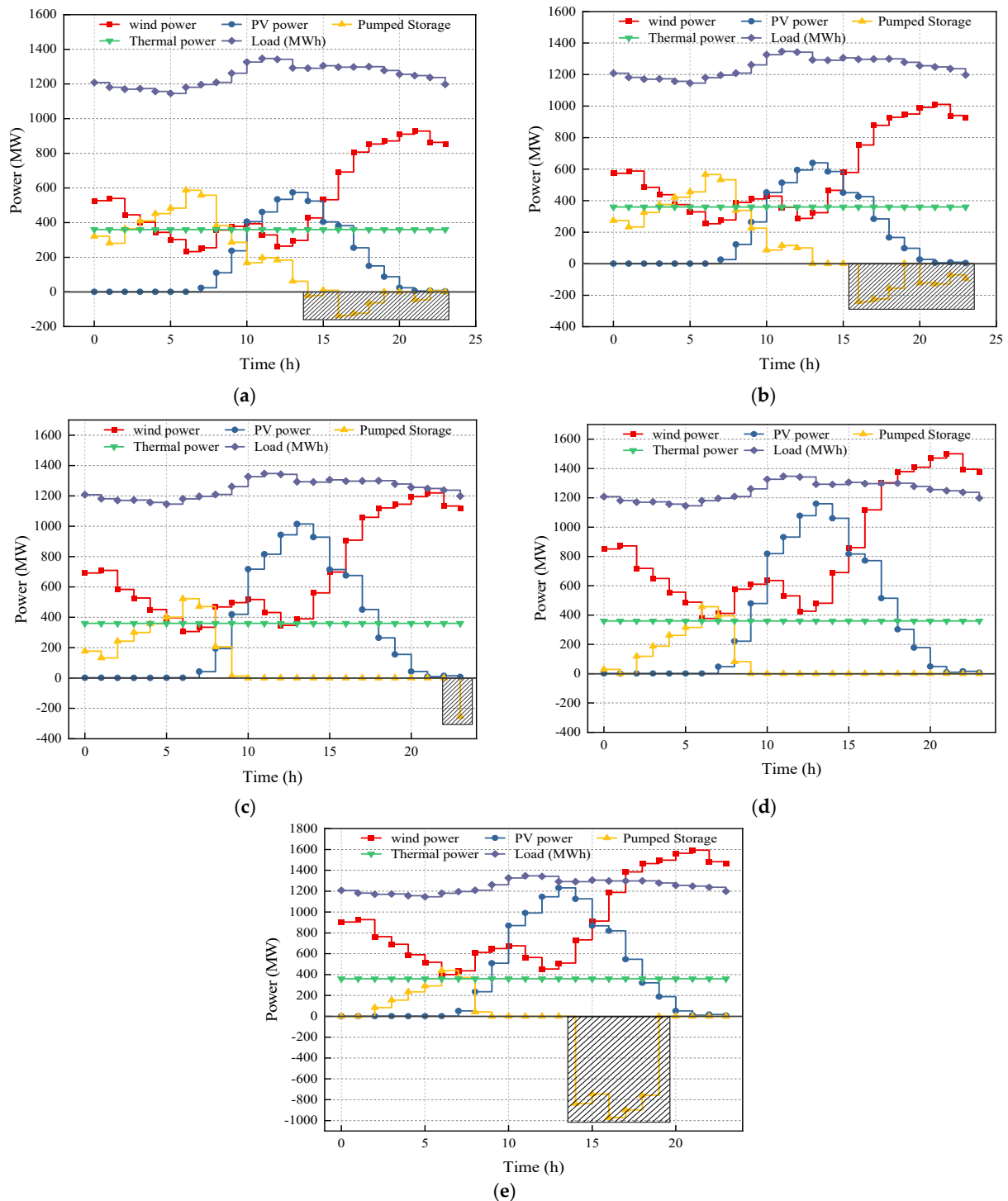


Figure 5. The day-ahead optimal scheduling output curve of each scenario. (a) Scenario 1 energy-abandonment rate = 1%; (b) scenario 2 energy-abandonment rate = 2%; (c) scenario 3 energy-abandonment rate = 3%; (d) scenario 4 energy-abandonment rate = 4%; (e) scenario 5 energy-abandonment rate = 5%.

Figure 5a–e shows the daily optimization scheduling results of these scenarios (1–5% energy-abandonment rate), where the system mainly increases the output of renewable

energy by increasing the installed capacity of renewable energy. As the installed capacity of renewable energy on the source side continues to increase, the energy-abandonment rate also increases. From the overall analysis of Figure 5, it can be concluded that when the penetration rate of renewable energy reaches over 50%, the conventional thermal power units connected to the system have been operating smoothly at the minimum output, while a high proportion of renewable energy connected to the system makes the thermal power units in the base load operation state. The system prioritizes the use of pumped storage units for peak shaving. As the penetration rate of renewable energy continues to increase, the capacity of pumped storage units participating in peak shaving also increases. The pumped storage units are in deep peak shaving mode to promote the consumption of high proportion renewable energy.

From Figure 5a, it can be seen that when the renewable energy penetration rate is around 50%, the typical daytime and evening wind power output on this typical day is relatively high. Therefore, the pumped storage units store energy at 15:00, 17–19:00, and 22:00, respectively, and the units start and stop five times a day, which is relatively frequent. From Figure 5b, it can be seen that when the wind and solar penetration rate is around 60%, the storage capacity of the pumped storage unit is about twice that of the penetration rate of 50%, the number of starts and stops of the pumped storage unit's output is significantly reduced, and the output of the peak shaving power supply is also more stable. From Figure 5c–e, it can be seen that when the penetration rate of renewable energy is around 70% and a very high proportion is connected to the system due to the extremely high proportion of wind and solar installed capacity, when the user's load demand remains unchanged, only the output of renewable energy can be met. Therefore, the pumped storage unit approaches the full power state when pumping and storing energy.

The relationship between daily operation cost and energy-abandonment rate can be calculated according to the system's daily dispatching results, as shown in Figure 6.

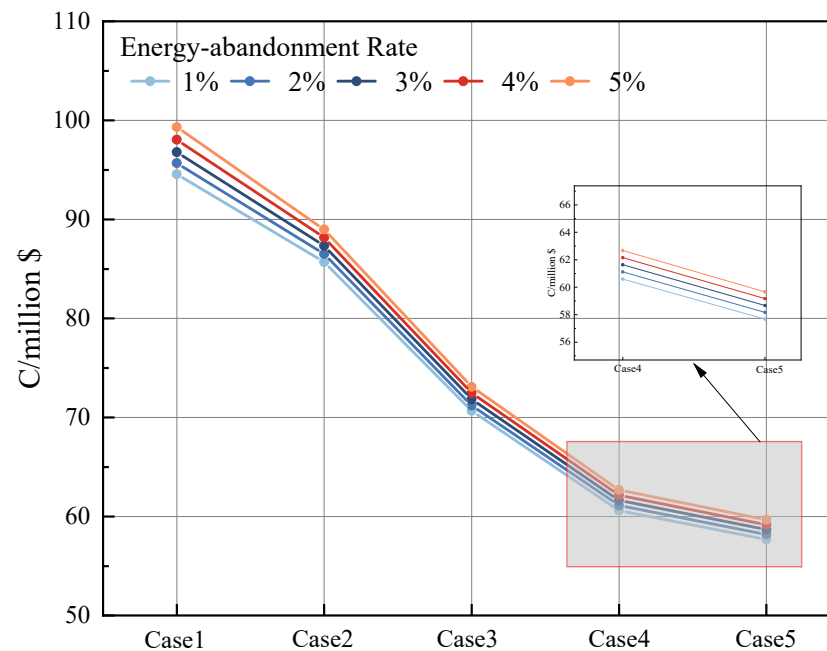


Figure 6. The relationship between energy-abandonment rate and system operating cost in different scenarios on the power source side.

From Figure 6, the operating cost increases with the increase in the energy-abandonment rate under the same installed capacity conditions. However, as the proportion of renewable energy access continues to increase, the daily operating cost of the system decreases by 40% compared to the initial scenario when the penetration rate of renewable energy reaches over 70%. Moreover, when the penetration rate of renewable energy in the system increases from

60% to 70%, the operating cost decreases the fastest. When the penetration rate of renewable energy in the system reaches over 70%, the impact of directly reducing the operating cost of the source side by increasing the installed capacity of renewable energy is relatively small. Therefore, when the penetration rate of renewable energy is between 60 and 70%, from the perspective of the power source side, the operating cost changes within a large range and the growth of renewable energy installation has a significant impact on the system operation. Under the same energy-abandonment rate, the daily operating cost decreases with the increase of renewable energy penetration rate.

According to research on the daily operating cost of the source side, there is a reasonable energy-abandonment interval. To further determine its accuracy, a reasonable energy-abandonment rate is introduced to predict the impact of future renewable energy penetration rates on the power generation system. A reasonable energy-abandonment rate is beneficial for reducing system consumption costs and improving system energy utilization efficiency. According to research calculations on the planned renewable energy installed capacity in 2025, the wind curtailment rate in the western region of China has decreased from 8.6% in 2020 to 7.8% in 2025 [25]. According to statistics from the National Energy Administration, the wind curtailment and light curtailment rates in the western region of China in 2022 were 6% and 2%, respectively. This article studies the reasonable energy-abandonment rate of the combined power generation system when the energy-abandonment rate is within 1~5%. The curves for calculating the system power side cost, grid side cost, and system comprehensive cost are shown in Figure 7.

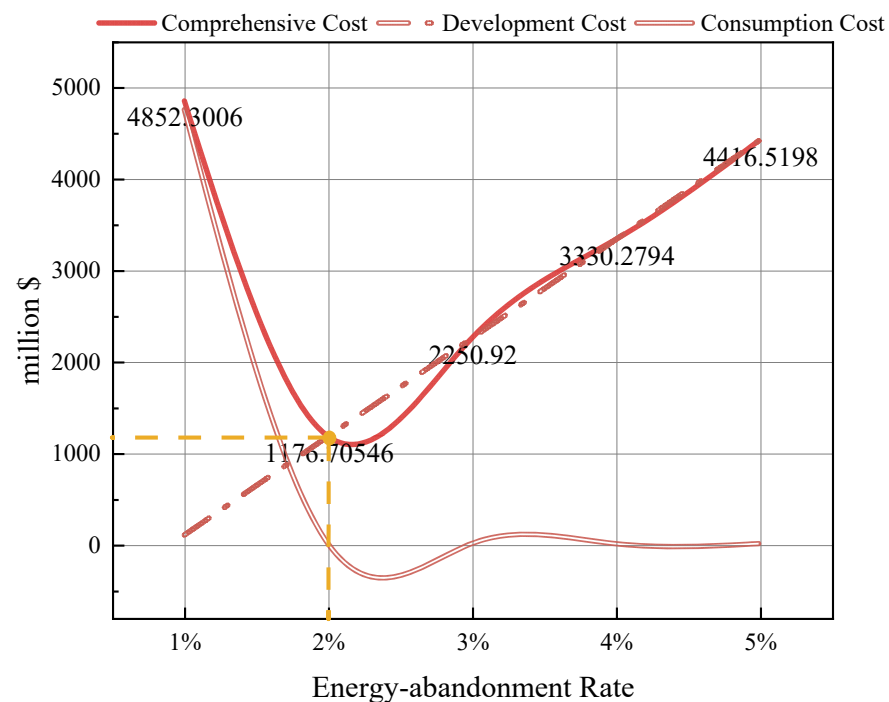


Figure 7. Calculation results of reasonable energy-abandonment rate points in the combined power generation system.

From Figure 7, the trend of the three sets of cost curves is basically consistent with the trend in the schematic diagram (in Figure 4). Among them, the newly installed cost of renewable energy on the power side shows a linear increase with the continuous increase of the energy-abandonment rate. The cost of renewable energy consumption on the grid side has shown a sharp downward trend due to the lack of new flexible adjustable power sources in the system. The lowest point of the total cost curve is the energy-abandonment rate of 2%, which is within the range of 1% to 5% in this study. When the energy-abandonment rate is 2%, the combined power generation system is considered the lowest comprehensive

cost on both sides of the source and grid, which is USD 11.77 million, of which the daily operating cost of the system is USD 0.87 million.

To further clarify the impact of a reasonable energy-abandonment rate on system optimization scheduling, the scheduling results for each scenario at a reasonable energy-abandonment rate of 2% are calculated as shown in Figure 8.

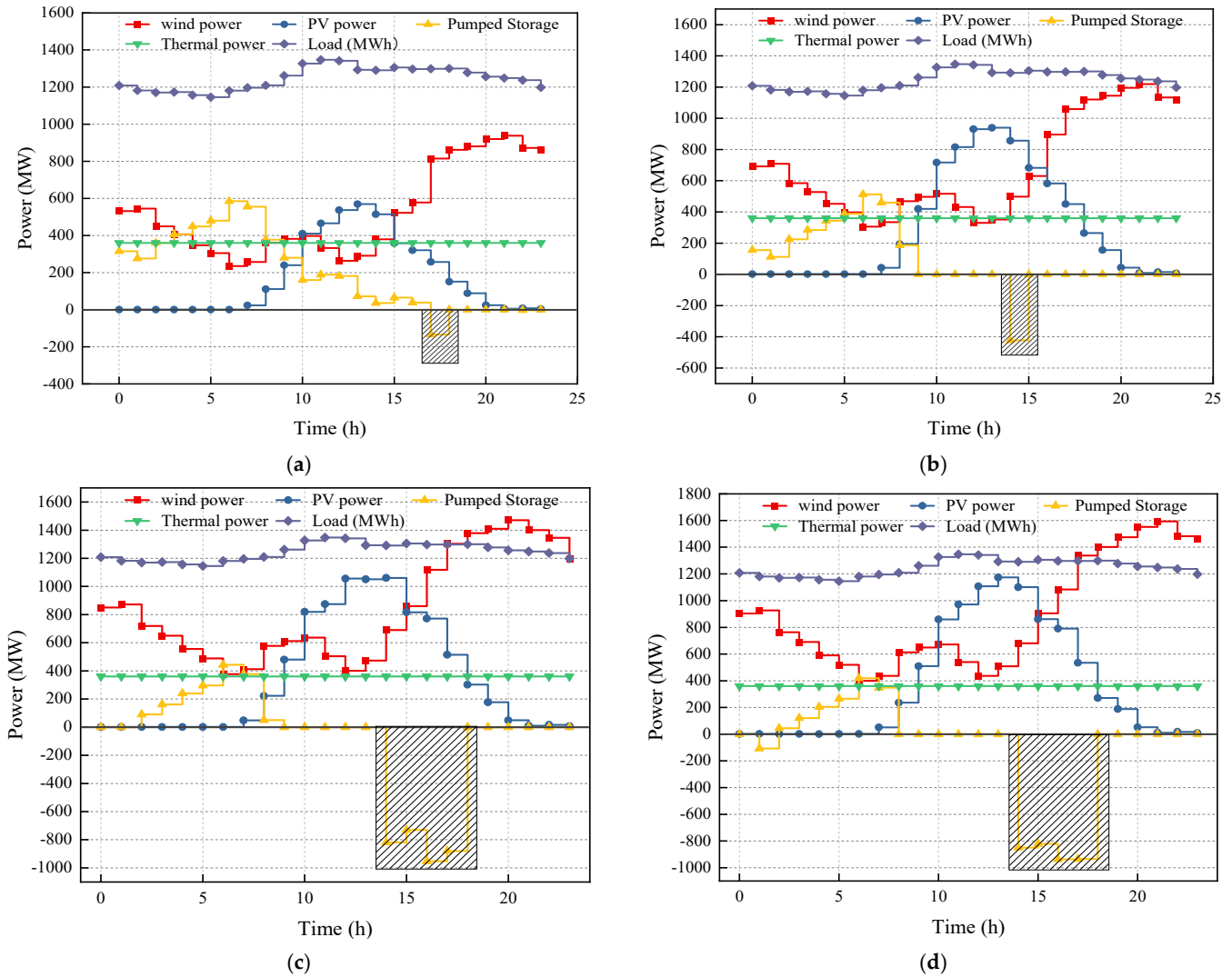


Figure 8. The reasonable energy-abandonment rate and the day-ahead optimal scheduling output diagram of each scenario. (a) Scenario 1 energy-abandonment rate = 2%; (b) scenario 3 energy-abandonment rate = 2%; (c) scenario 4 energy-abandonment rate = 2%; (d) scenario 5 energy-abandonment rate = 2%.

From the analysis of Figure 8a–d, it can be concluded that compared to the energy-abandonment rate set in Figure 8, the overall startup and shutdown frequency of pumped storage units under a reasonable energy-abandonment rate is 1–2 times a day, greatly reducing the impact of frequent startup and shutdown of units on system operation. When the renewable energy permeability is between 50 and 60%, pumped storage units only store a small amount of energy in a short period in the afternoon during a typical day. When the renewable energy permeability is above 70%, Pumped storage units are typically at high-power energy storage from 14:00 to 19:00 during a typical day, and the units mainly play a role in active power regulation in the system.

The analysis of reasonable energy-abandonment rate within the system should also consider the degree to which the combined output of renewable energy tracks the load. The relationship between the wind–PV power output curve and load is shown in Figure 9.

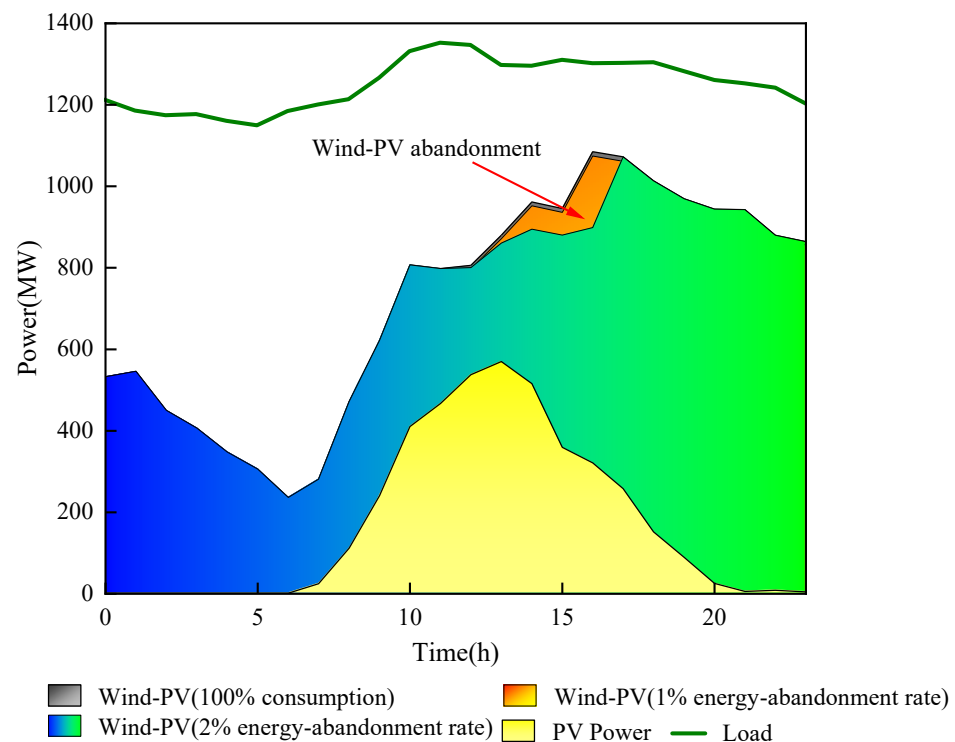


Figure 9. Comparison diagram of wind–PV combined output in scenario 4.1 considering reasonable energy-abandonment.

As shown in Figure 9, taking scenario 1 as an example, when the wind–solar output power is fully absorbed, there is a significant lag in the load tracking ability compared to when it is at a reasonable energy-abandonment rate. Generally speaking, wind power and load exhibit a significant anti-peak characteristic, while in the western region, wind power output is relatively large on summer evenings, and the anti-peak characteristic is less obvious. The combined output of wind–PV can meet the local load demand. When the energy-abandonment rate of renewable energy is 1%, it can be seen that its output curve is relatively consistent with that of complete absorption, and its load-tracking ability is poor. However, when the system’s renewable energy output is at a reasonable energy-abandonment rate, its load tracking ability is significantly enhanced, the abandoned energy is concentrated at noon, and the system operation is in a better state.

The correlation between reasonable energy-abandonment rate and system operating cost is also significant. The relationship curve between reasonable energy-abandonment rate, set energy-abandonment rate, and daily operating cost for each scenario is shown in Figure 10.

From Figure 10, it can be seen that the cost of scenario 1 under a reasonable energy-abandonment rate is slightly higher than that of the 1% energy abandonment scenario. The increase in abandoned electricity inevitably leads to an increase in system operating costs. However, according to the analysis in Figure 8, it improves system stability and load-tracking intensity. As the proportion of renewable energy access increases, the impact of reasonable energy-abandonment rate on daily operating costs shows a class exponential relationship, with a gradual increase in the decrease. When the penetration ratio of renewable energy is between 50 and 60%, the decrease is 2.3%, while when the system is connected to the ultra-high proportion of renewable energy (>70%), the decrease jumps to 4.2%. There-

fore, for the ultra-high proportion of renewable energy access systems, it is more important to keep the system operating at the calculated reasonable energy-abandonment rate.

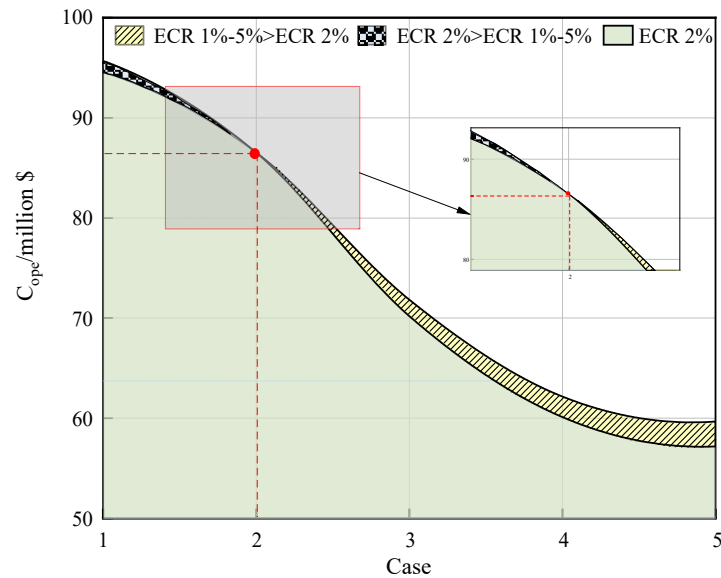


Figure 10. Comparison of operating costs of various scenarios considering the reasonable energy-abandonment rate.

5. Conclusions

This paper presents a day-ahead optimized dispatching model aimed at minimizing generalized load fluctuations, operating costs, and carbon emissions of a combined power generation system comprising pumped storage, wind, solar, and thermal sources. A clustering algorithm is used to extract typical daily data from the source and load sides of the pumped storage energy base in the western region of China, and the reasonable energy-abandonment operation of the combined power generation system is analyzed considering the comprehensive cost. A reasonable energy-abandonment rate is beneficial for reducing system consumption costs and improving system energy utilization efficiency. The main conclusions are as follows:

- (1) The improved K-means clustering algorithm is utilized to discern characteristic days for wind and solar power generation across the four seasons at the energy base in the western region of China. Distinct days, including April 17 for spring, July 26 for summer, October 16 for autumn, and January 17 for winter, have been identified as representative. Notably, the summer day exhibits the highest daily load fluctuation and the strongest wind–solar synergy, making it an optimal focal point for probing the regulatory capacity of pumped storage. Consequently, scenario analyses will concentrate on the load dynamics of this identified typical summer day.
- (2) At a renewable energy penetration of 60–70%, the development cost on the source side is significantly influenced by installed capacity, with consumption costs exhibiting a marked decrease. A reasonable energy curtailment rate of 2% yields the minimum comprehensive cost of USD 11.77 million for the integrated generation system. These findings provide valuable insights for renewable energy expansion, grid planning, and operational scheduling at the energy base in the western region of China.
- (3) Due to the fluctuating characteristics of renewable energy, it is often unrealistic to pursue the complete consumption of renewable energy in the case of ultra-high proportion access. It is more instructive to consider the optimal operation of a combined power generation system under the reasonable energy-abandonment rate of 2%, which can make its electricity peak shaving, system stability perform better, and lower daily operating costs by 4.2%.

Author Contributions: Methodology, J.Y. and C.L.; Validation, J.Y., C.L., P.G. and F.C.; Formal analysis, H.Z. and P.G.; Investigation, H.Z., R.J., F.G. and F.C.; Resources, C.L. and P.G.; Data curation, H.Z., J.Y. and J.L.; Writing—original draft, H.Z., J.Y. and C.L.; Writing—review and editing, P.G., J.L., R.J., J.H., F.G. and F.C.; Visualization, H.Z. and J.L.; Supervision, J.L., R.J. and J.H.; Project administration, J.H. and F.G.; Funding acquisition, R.J., J.H., F.G. and F.C. All authors have read and agreed to the published version of the manuscript.

Funding: This work was supported by the National Natural Science Foundation of China (Grant No. 52309119, 52306051, U2243216, 51839010), the China Postdoctoral Science Foundation (Grant No. 2022M722560), and the Natural Science Basic Research Program of Shaanxi (Program No. 2023-JC-QN-0412).

Data Availability Statement: The original contributions presented in the study are included in the article, further inquiries can be directed to the corresponding authors.

Conflicts of Interest: Authors Jun Liu, Ruibao Jin, Jing Hu were employed by the company Henan Jiaotou Jiaozheng Expressway Co., Ltd. Author Fengyuan Gan was employed by the company Henan Province Highway Engineering Bureau Group Co., Ltd. Author Fei Cao was employed by the company Henan Railway Construction & Investment Group Co., Ltd. The remaining authors declare that the research was conducted in the absence of any commercial or financial relationships that could be construed as a potential conflict of interest.

References

1. Xu, D.; Tao, L.; Xiang, Y.; Meng, X.; Li, X.R.; Hou, J.; Xu, Y.H.; Wang, F.L. Assessing the carbon emission reduction effect of flexibility option for integrating variable renewable energy. *Energy Econ.* **2024**, *132*, 107461.
2. Sikandar, A.Q.; Hessah, A.; Furqan, T.; Luluwah, A. Incentives and strategies for financing the renewable energy transition: A review. *Energy Econ.* **2021**, *7*, 3590–3606.
3. Jian, Y.J.; Yu, H.C.; Xing, M.Y. The blue treasure of hydrogen energy: A research of offshore wind power industry policy in China. *Int. J. Hydrogen Energy* **2024**, *62*, 99–108.
4. Qusay, H.; Ahmed, K.N.; Ali, K.A.; Patrik, V.; Ahmad, A.T.; Emad, M.A.; Ayesha, A.; Hassan, F.F.; Sameer, A.; Saoud, C.M.; et al. Mapping Europe renewable energy landscape: Insights into solar, wind, hydro, and green hydrogen production. *Technol. Soc.* **2024**, *77*, 102535.
5. Zwalnan, S.J.; Yousif, A.A.; Nanchen, N.C.; Baiman, C. An open-loop hybrid photovoltaic solar thermal evacuated tube energy system: A new configuration to enhance techno economic of conventional photovoltaic solar thermal system. *J. Build.* **2024**, *82*, 108000.
6. Toru, O.; Yasuyuki, S.; Taketsune, N. Concept study of wind power utilizing direct thermal energy conversion and thermal energy storage. *Renew. Energy* **2015**, *83*, 332–338.
7. Kok, S.W.; Zhen, X.P.; Jan, T.; Petar, S.V.; Cheng, T.C.; Jiří, J.K.; Chew, T.L. Recent advances in urban green energy development towards carbon emissions neutrality. *Energy* **2023**, *267*, 126502.
8. Xiang, Q.Y.; Lai, S.L. Renewable energy transition and its implication on natural resource management for green and sustainable economic recovery. *Resour. Policy* **2024**, *89*, 104624.
9. Rehman, S.; Al-Hadhrami, L.M.; Alam, M.M. Pumped hydro energy storage system: A technological review. *Renew. Sustain. Energy Rev.* **2015**, *44*, 586–598. [[CrossRef](#)]
10. Wang, Z.; Fang, G.; Wen, X.; Tan, Q.F.; Zhang, P.; Liu, Z.H. Coordinated operation of conventional hydropower plants as hybrid pumped storage hydropower with wind and photovoltaic plants. *Energy Convers. Manag.* **2023**, *277*, 116654. [[CrossRef](#)]
11. Nasir, J.; Javed, A.; Ali, M.; Ullah, K.; Kazmi, S.A. Capacity optimization of pumped storage hydropower and its impact on an integrated conventional hydropower plant operation. *Appl. Energy* **2022**, *323*, 119561. [[CrossRef](#)]
12. Peng, Z.; Chen, X.; Yao, L. Research status and future of hydro-related sustainable complementary multi-energy power generation. *Sustain. Futures* **2021**, *3*, 100042. [[CrossRef](#)]
13. Wang, Y.; Fang, G. Joint Operation Modes and Economic Analysis of Nuclear Power and Pumped Storage Plants under Different Power Market Environments. *Sustainability* **2022**, *14*, 9128. [[CrossRef](#)]
14. Liu, B.; Zhou, J.; Guo, W.; Li, M.Y. A many-objective optimization strategy for unified optimal operation of pumped storage hydropower station under multiple load rejection conditions. *Energy Sustain. Dev.* **2023**, *74*, 34–49. [[CrossRef](#)]
15. Li, X.D.; Yang, W.J.; Zhao, Z.G.; Wang, R.; Yin, X.X. Advantage of priority regulation of pumped storage for carbon-emission-oriented co-scheduling of hybrid energy system. *J. Energy Storage* **2023**, *58*, 106400. [[CrossRef](#)]
16. Cavazini, G.; Benato, A.; Pavesi, G.; Ardizzon, G. Techno-economic benefits deriving from optimal scheduling of a Virtual Power Plant: Pumped hydro combined with wind farms. *J. Energy Storage* **2021**, *37*, 102461. [[CrossRef](#)]
17. Psarros, G.N.; Papathanassiou, S.A. Internal dispatch for RES-storage hybrid power stations in isolated grids. *Renew. Energy* **2020**, *147*, 2141–2150. [[CrossRef](#)]

18. Makhdoomi, S.; Askarzadeh, A. Daily performance optimization of a grid-connected hybrid system composed of photovoltaic and pumped hydro storage (PV/PHS). *Renew. Energy* **2020**, *159*, 272–285. [[CrossRef](#)]
19. Makhdoomi, S.; Askarzadeh, A. Optimizing operation of a photovoltaic/diesel generator hybrid energy system with pumped hydro storage by a modified crow search algorithm. *J. Energy Storage* **2020**, *27*, 101040. [[CrossRef](#)]
20. Diab, A.A.Z.; Sultan, H.M.; Kuznetsov, O.N. Optimal sizing of hybrid solar/wind/hydroelectric pumped storage energy system in Egypt based on different meta-heuristic techniques. *Environ. Sci. Pollut. Res.* **2020**, *27*, 32318–32340. [[CrossRef](#)] [[PubMed](#)]
21. Liu, X.; Li, N.; Mu, H.; Li, M.; Liu, X.X. Techno-energy-economic assessment of a high capacity offshore wind-pumped-storage hybrid power system for regional power system. *J. Energy Storage* **2021**, *41*, 102892. [[CrossRef](#)]
22. Zhang, Y.; Ma, C.; Yang, Y.; Pang, X.L.; Lian, J.J.; Wang, X. Capacity configuration and economic evaluation of a power system integrating hydropower, solar, and wind. *Energy* **2022**, *259*, 125012. [[CrossRef](#)]
23. Bertsiou, M.M.; Baltas, E. Management of energy and water resources by minimizing the rejected renewable energy. *Sustain. Energy Technol. Assess.* **2022**, *52*, 102002. [[CrossRef](#)]
24. Li, L.; Wang, B.; Jiao, K.; Ni, M.; Du, Q.; Liu, Y.L.; Li, B.; Ling, G.W.; Wang, C.S. Comparative techno-economic analysis of large-scale renewable energy storage technologies. *EAI* **2023**, *14*, 100282. [[CrossRef](#)]
25. Wang, R.; Yang, W.J.; Lo, X.D.; Zhao, Z.G.; Zhang, S.S. Day-ahead multi-objective optimal operation of Wind–PV–Pumped Storage hybrid system considering carbon emissions. *Energy Rep.* **2022**, *8*, 1270–1279. [[CrossRef](#)]
26. Wang, J.S.; Yin, X.X.; Liu, Y.K.; Cai, W.D. Optimal design of combined operations of wind power-pumped storage-hydrogen energy storage based on deep learning. *Electr. Power Syst. Res.* **2023**, *218*, 109216. [[CrossRef](#)]
27. Xu, X.; Hu, W.H.; Cao, D.; Huang, Q.; Chen, C.; Chen, Z. Optimized sizing of a standalone PV-wind-hydropower station with pumped-storage installation hybrid energy system. *Renew. Energy* **2020**, *147*, 1418–1431. [[CrossRef](#)]
28. Shabani, M.; Dahlquist, E.; Wallin, F.; Yan, J.Y. Techno-economic comparison of optimal design of renewable-battery storage and renewable micro pumped hydro storage power supply systems: A case study in Sweden. *Appl. Energy* **2020**, *279*, 115830. [[CrossRef](#)]
29. Mirzapour, O.; Rui, X.; Sahraei-Ardakani, M. Transmission impedance control impacts on carbon emissions and renewable energy curtailment. *Energy* **2023**, *278*, 127741. [[CrossRef](#)]
30. Yasuda, Y.; Bird, L.; Carlini, E.M.; Eriksen, P.B.; Estanqueiro, A.; Flynn, D.; Fraile, D.; Lazaro, E.G.; Martin-Martinez, S.; Hayashi, D.; et al. C-E (curtailment—Energy share) map: An objective and quantitative measure to evaluate wind and solar curtailment. *Renew. Sustain. Energy Rev.* **2022**, *160*, 112212. [[CrossRef](#)]
31. Wang, Y.H.; Li, N.; Yuan, B.; Zhang, F.Q.; Feng, J.S. Discussion on the Reasonable Curtailment Problems in Highly Renewable Power System Planning. *Electr. Power* **2017**, *50*, 8–14.
32. Gao, L.; Su, X.Y.; Liu, S.Y. Study on Reasonable Curtailment Rate of Renewables under Certain Renewable Energy Consumption Quota Obligation. *Electr. Power* **2020**, *53*, 136–142.
33. Li, J.L.; Zhao, Z.W.; Xu, D.; Li, P.Q.; Liu, Y.; Mahmud, M.A.; Chen, D.Y. The potential assessment of pump hydro energy storage to reduce renewable curtailment and CO₂ emissions in Northwest China. *Renew. Energy* **2023**, *212*, 82–96. [[CrossRef](#)]

Disclaimer/Publisher’s Note: The statements, opinions and data contained in all publications are solely those of the individual author(s) and contributor(s) and not of MDPI and/or the editor(s). MDPI and/or the editor(s) disclaim responsibility for any injury to people or property resulting from any ideas, methods, instructions or products referred to in the content.